

# Cautious Model Predictive Control using Gaussian Process Regression

Lukas Hewing, Melanie N. Zeilinger

**Abstract**—Gaussian process (GP) regression has been widely used in supervised machine learning for its flexibility and inherent ability to describe uncertainty in the function estimation. In the context of control, it is seeing increasing use for modeling of nonlinear dynamical systems from data, as it allows the direct assessment of residual model uncertainty. We present a model predictive control (MPC) approach that integrates a nominal linear system with an additive nonlinear part of the dynamics modeled as a GP. Approximation techniques for propagating the state distribution are reviewed and the benefits of considering feedback in the prediction is demonstrated. We describe a principled way of formulating the chance constrained MPC problem, which takes into account residual uncertainties provided by the GP model to enable cautious control. Efficient computation with state-of-the-art solvers is discussed and simulation examples demonstrate the feasibility of the approach for systems with sub-second sampling times.

**Index Terms**—Model Predictive Control, Gaussian Processes, Stochastic Model Predictive Control

## I. INTRODUCTION

Nonlinearities are inherent in almost all real world control systems. While linear models often perform well in a neighborhood of the trim point, unmodeled nonlinear effects deteriorate performance in a larger operating space. Modeling nonlinear effects is typically a time-consuming and complex endeavor, both when directly identifying the nonlinearity and when generating a map of linearized models at different operating points. In this context, learning methods for automatically identifying dynamical models from data have gained significant attention in the past years [1], [2] and more recently for robotic applications [3], [4]. In particular nonparametric methods, which have seen wide success in machine learning, offer significant potential for control [5]. The appeal of using Gaussian Process (GP) regression for model learning stems from the fact that it requires little prior process knowledge and directly provides a measure of residual model uncertainty. This paper discusses the use of GP models and their uncertainty measure for cautious model predictive control (MPC).

In predictive control, GPs were successfully applied to improve control performance when learning periodic time-varying disturbances [6]. The task of learning the system dynamics as opposed to disturbances, however, imposes the challenge of propagating probability distributions of the state over the prediction horizon of the controller. Efficient methods to evaluate GPs for Gaussian inputs have been developed in

[7], [8], [9]. By successively employing these approximations at each prediction time step, predictive control with GP dynamics has been presented in [10]. In [11] a piecewise linear approximate explicit solution for the MPC problem of a combustion plant was presented. Application of a one-step MPC with a GP model to a mechatronic system was demonstrated in [12] and the use for fault-tolerant MPC was presented in [13]. A constrained tracking MPC for robotic applications, which uses a GP to improve the dynamics model from measurement data, was shown in [14]. A variant of this was realized in [15], where uncertainty of the GP prediction is robustly taken into account using confidence bounds. Although the concept of combining GP models with MPC has therefore been addressed in previous work, practical aspects of posing and solving the resulting optimization problem are intricate and require a combination of various results.

The goal of this paper is to provide an overview of existing techniques and propose extensions for deriving a systematic and efficiently solvable approximate formulation of the MPC problem with a GP model, which incorporates constraints and takes into account the model uncertainty for cautious control. In particular, we focus on dynamical models consisting of a linear state space model augmented by nonlinear terms. This corresponds to a common scenario in controller design, where linear model approximations are often available, and only specific nonlinear effects need to be identified from data. For example, most dynamical models derived from physical laws include an integrator chain, which can be directly represented in the linear dynamics and for which no nonlinear and uncertainty model has to be learned from data.

The paper makes the following contributions. A review and compact summary of approximation techniques for propagating GP dynamics and uncertainties is provided and extended to the additive combination with linear dynamics. This enables the principled formulation of chance constraints on the resulting state distributions. The introduction of a nominal linear system furthermore enables the design of linear ancillary controllers, which are incorporated in the MPC problem to limit uncertainty growth over the prediction and reduce conservatism of the cautious controller. In addition, the GP model learning can be reduced to a subspace of states and inputs, decoupling the dimensions of the system and the learned model. This is crucial in order to make the computationally expensive GP approach practically feasible for medium- and potentially even large-scale systems. We finally demonstrate the proposed approach in simulation examples for a 4th-order system for which average computation times of less than four milliseconds are achieved.

The authors are with the Institute for Dynamic Systems and Control, ETH Zürich, Zürich CH-8092, Switzerland (e-mail: lhewing@ethz.ch; mzeilinger@ethz.ch)

This work was supported by the Swiss National Science Foundation under grant no. PP00P2 157601 / 1.

## II. PRELIMINARIES

### A. Notation

The  $i$ -th element of a vector  $x$  is denoted as  $[x]_i$ . Similarly  $[M]_{ij}$  denotes element  $ij$  of a matrix  $M$ ,  $[M]_{\cdot i}$ ,  $[M]_i$  its  $i$ -th column or row, respectively.  $\text{diag}(x)$  is a diagonal matrix with entries given by the vector  $x$ .  $[X_1, X_2]$  refers to vertical matrix or vector concatenation,  $[X_1 \ X_2]$  horizontal concatenation.  $\|x\|_M^2$  is the squared Euclidean norm weighted by  $M$ , i.e.  $x^T M x$ . We use boldface to emphasize stacked quantities, e.g. a collection of vector-valued data in matrix form.  $\nabla_x f(z)$  denotes the gradient of  $f$  w.r.t.  $x$  evaluated at  $z$ , the subscript is dropped if clear from the context.

$x \sim \mathcal{N}(\mu, \Sigma)$  is a normally distributed vector  $x$  with mean  $\mu$  and variance  $\Sigma$ .  $\mathbb{E}(x)$  is the expected value of  $x$ ,  $\text{cov}(x, y)$  the covariance between vectors  $x$  and  $y$ , and the variance  $\text{var}(x) = \text{cov}(x, x)$ .  $P(E)$  denotes the probability of an event  $E$ .

Subscripts are typically used for time indices and superscripts otherwise, e.g.  $\mu_i^x$  is the mean of the variable  $x$  at time  $i$ . Similarly,  $x_{i|k}$  refers to the  $i$ -th prediction time step for the system state made at time instance  $k$ . The index  $k$  is omitted if clear from the context.

### B. Problem formulation

We consider the control of dynamical systems that can be represented by the discrete-time model

$$x_{k+1} = Ax_k + Bu_k + B^d (g(x_k, u_k) + w_k) , \quad (1)$$

composed of a linear part and additive nonlinear dynamics, where  $x_k \in \mathbb{R}^{n_x}$  are the system states and  $u_k \in \mathbb{R}^{n_u}$  the control inputs at time  $k$ . For brevity, we use  $z_k = [x_k, u_k] \in \mathbb{R}^{n_z}$ , when convenient. The function  $g : \mathbb{R}^{n_z} \rightarrow \mathbb{R}^{n_d}$  describes nonlinearities of the system, which are assumed to lie in the subspace spanned by  $B^d$ , but are otherwise unknown. We consider i.i.d. uncorrelated process noise on the nonlinearity  $w_k \sim \mathcal{N}(0, \Sigma^w)$ , with diagonal variance matrix  $\Sigma^w$ .

The system is constrained by polytopic state and input constraints of the form

$$\mathcal{X} := \{x \in \mathbb{R}^{n_x} | H^x x \leq b^x\} , \quad (2a)$$

$$\mathcal{U} := \{u \in \mathbb{R}^{n_u} | H^u u \leq b^u\} , \quad (2b)$$

with  $b^x \in \mathbb{R}^p$  and  $b^u \in \mathbb{R}^l$ . By considering process noise with infinite support, the constraints can only be satisfied in a probabilistic manner and are formulated as chance constraints, i.e., by constraining the probability of violation

$$P(x_k \in \mathcal{X}) > 1 - \epsilon^x , \quad (3a)$$

$$P(u_k \in \mathcal{U}) > 1 - \epsilon^u , \quad (3b)$$

where  $\epsilon^x$ ,  $\epsilon^u$  capture the associated probability of violation.

**Remark 1.** *The extension of this approach to time-varying linear systems is straightforward but omitted for clarity.*

### C. Gaussian Process Regression

Gaussian process regression is a nonparametric data-driven framework for nonlinear regression. A scalar GP is a probability distribution over functions, such that every finite sample

of function values is jointly Gaussian distributed. It is fully specified by its prior mean function  $m(\cdot)$  and a positive semidefinite kernel function  $k(\cdot, \cdot)$ . While the prior mean function specifies knowledge of the mean at a test point prior to observing data, the kernel function expresses the covariance between data points. Given data, the posterior distribution at a test point is then found by Gaussian conditioning on the data and is greatly influenced by the choice of kernel function  $k(\cdot, \cdot)$ . For the case of the squared exponential kernel, this has been shown to offer universal function approximation [16].

We apply Gaussian processes regression to infer the noisy vector-valued function  $g(z) + w$  of the system dynamics from previously collected measurement data of states and inputs  $\{(x_j, u_j) | j = 1, \dots, M+1\}$ . State-input pairs form the input data to the GP and the corresponding output data is obtained as the deviation from the linear system model:

$$\Delta_j = \text{argmin} \left\| x_{j+1} - [A \ B] z_j - B^d \tilde{\Delta}_j \right\| . \quad (4)$$

The data set of the GP is therefore given by

$$\mathcal{D} = \{(z_j, \Delta_j) | j = 1, \dots, M\} , \quad (5)$$

with noise on output data given by  $w \sim \mathcal{N}(0, \Sigma^w)$ .

We define  $n_d$  scalar GPs for output dimensions  $a = 1 \dots n_d$  with common input data  $\mathbf{z} = [z_1^T, \dots, z_M^T]$  and individual scalar outputs  $\mathbf{\Delta}^a = [[\Delta_1]_a, \dots, [\Delta_M]_a]$  with noise given by the corresponding entry  $[\Sigma^w]_{aa}$ . This ensures conditional independence of the individual scalar GP distributions given  $z$ . With  $n_d$  individual mean and kernel functions  $\mathbf{m}(z) = [m^1(z), \dots, m^{n_d}(z)]$  and  $\mathbf{k}(z, z') = [k^1(z, z'), \dots, k^{n_d}(z, z')]$  the posterior distribution in each dimension is given by a Gaussian with mean and variance

$$\mu^{d,a}(z) = m^a(z) + k^a(\mathbf{z}, z)^T (K^a)^{-1} (\mathbf{\Delta}^a - \mathbf{1} m^a(z)) , \quad (6a)$$

$$\Sigma^{d,a}(z) = k^a(z, z) - k^a(\mathbf{z}, z)^T (K^a)^{-1} k^a(\mathbf{z}, z) + [\Sigma^w]_{aa} . \quad (6b)$$

Here  $K^a = k^a(\mathbf{z}, \mathbf{z}) + I[\Sigma^w]_{aa}$  is the kernel gram matrix of the input data  $\mathbf{z}$  plus measurement noise,  $k^a(\mathbf{z}, z)$  the kernel gram matrix of the input data with respect to the test point  $z$  and  $\mathbf{1} = [1, \dots, 1]$ . The posterior distribution of the multivariate GP is finally given by the vector of the scalar posterior mean values and a diagonal matrix composed of the scalar posterior variances

$$\mu^d(z) = [\mu^{d,1}(z), \dots, \mu^{d,n_d}(z)] , \quad (7a)$$

$$\Sigma^d(z) = \text{diag}([\Sigma^{d,1}(z), \dots, \Sigma^{d,n_d}(z)]) , \quad (7b)$$

where  $\mu^d : \mathbb{R}^{n_z} \rightarrow \mathbb{R}^{n_d}$  and  $\Sigma^d : \mathbb{R}^{n_z} \rightarrow \mathcal{S}^{n_d}$ , and  $\mathcal{S}$  is the set of positive diagonal real matrices. We denote this GP approximation of  $g(z)$  by  $d(z)$ , with

$$d(z) \sim \mathcal{GP}(\mathbf{m}(z), \mathbf{k}(z, z') | \mathcal{D}) . \quad (8)$$

## III. MPC CONTROLLER DESIGN

In this paper, we consider the design of an MPC controller for system (1) using a GP approximation of the nonlinearity:

$$x_{i+1|k} = Ax_{i|k} + Bu_{i|k} + B^d d(z_{i|k}) . \quad (9)$$

At each time step, the GP approximation evaluates to a stochastic distribution according to the residual model uncertainty and process noise, which is then propagated forward in time. A stochastic MPC formulation allows the principled treatment of chance constraints on both inputs and states arising from these distributions. A common issue in stochastic and robust MPC is the lack of feedback in the prediction when optimizing over a control input sequence. This often leads to a rapid growth in uncertainty over the prediction horizon and conservative control [17], [18]. To alleviate this problem, one can instead optimize over input policies  $\Pi(x) = \{\pi_i(x)\}$ , also known as feedback MPC [19].

The resulting optimization problem is given by

$$\min_{\Pi(x)} l_f(x_{N|k}) + \sum_{i=0}^{N-1} l(x_{i|k}, u_{i|k}) \quad (10a)$$

$$\text{s.t. } x_{0|k} = x_0 \quad (10b)$$

$$x_{i+1|k} = Ax_{i|k} + B\pi_i(x_{i|k}) + B^d d(z_{i|k}) \quad (10c)$$

$$u_{i|k} = \pi_i(x_{i|k}) \quad (10d)$$

$$P(x_{i|k} \in \mathcal{X}) > 1 - \epsilon^x \quad (10e)$$

$$P(u_{i|k} \in \mathcal{U}) > 1 - \epsilon^u, \quad (10f)$$

for all  $i = 0, \dots, N-1$  and appropriate terminal cost  $l_f(x_{N|k})$  and stage cost  $l(x_{i|k}, u_{i|k})$ . In the form (10), the optimization problem is generally intractable. In the following sections, we present techniques for deriving an efficiently solvable approximation of problem (10).

### A. Ancillary State Feedback Controller

Optimization over general feedback policies  $\Pi(x)$  is an infinite dimensional optimization problem and not computationally tractable. A common approach that integrates well in the presented framework is to restrict the policy class to an ancillary linear state feedback controller

$$\pi_i(x_{i|k}) = K_i x_{i|k} + v_i, \quad (11)$$

with a pre-selected gain  $K_i$ , and optimize over  $v_i$ , the deviation from the linear control law. Assuming an accurate linear representation of the system around the set point, such that  $g(0,0) = 0$  and  $\nabla g(0,0) = 0$ , a linear state feedback controller designed for the nominal linear system will also perform well on the nonlinear system in a neighborhood of the origin and will improve the predictions by introducing feedback. By employing methods from robust linear control, such as  $H_\infty$  control, this neighborhood can be enlarged [20].

In Fig. 1 the effect of state feedback on the propagation of uncertainty is exemplified. It shows the evolution over time of a double integrator with a quadratic friction term inferred by a GP. The right plot displays mean and  $2\text{-}\sigma$  variance of a number of trajectories from Monte Carlo simulations of the system. Mean and variance under an open-loop control sequence derived from a linear quadratic infinite time optimal control problem are shown in red. The results with a corresponding LQR feedback law applied in closed-loop are shown in blue. As evident, open-loop input sequences can lead to rapid growth of uncertainty in the prediction, and

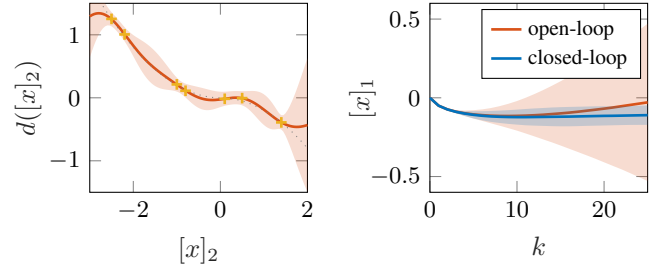


Fig. 1. Propagation of uncertainty for double integrator with GP trained on a nonlinear friction term. The left plot displays the GP with  $2\text{-}\sigma$  confidence bound, while the right plot shows the mean and  $2\text{-}\sigma$  variance of Monte Carlo simulations of the system under an open-loop control sequence and closed-loop state feedback control.

thereby cause conservative control actions in the presence of chance constraints. Linear ancillary state feedback controllers are therefore commonly employed in stochastic and robust MPC [21] and can be similarly integrated in the proposed MPC problem using a combined linear and GP model to improve the prediction.

### B. Uncertainty Propagation as Normal Distributions

Because of stochastic process noise and the representation of the nonlinearity by a GP, future predicted states are given as stochastic distributions. Evaluating the posterior of a GP from an input distribution is intractable in this case and the resulting distribution is not Gaussian [7]. A computationally effective approach is to approximate state, control input and GP as jointly Gaussian distributed at every time step:

$$\begin{aligned} \begin{bmatrix} x_{i|k} \\ u_{i|k} \\ d_{i|k} \end{bmatrix} &\sim \mathcal{N}(\mu_i, \Sigma_i) = \mathcal{N}\left(\begin{bmatrix} \mu_i^z \\ \mu_i^d \end{bmatrix}, \begin{bmatrix} \Sigma_i^z & \Sigma_i^{zd} \\ \star & \Sigma_i^d \end{bmatrix}\right) \\ &= \mathcal{N}\left(\begin{bmatrix} \mu_i^x \\ K\mu_i^x + v_i \\ \mu_i^d \end{bmatrix}, \begin{bmatrix} \Sigma_i^x & \Sigma_i^x K_i^T & \Sigma_i^{xd} \\ \star & K_i \Sigma_i^x K_i^T & \Sigma_i^{ud} \\ \star & \star & \Sigma_i^d \end{bmatrix}\right), \end{aligned} \quad (12)$$

where  $\star$  denotes terms given by symmetry. This facilitates simple update equations for state mean and variance based on linear transformations of Gaussian distributions

$$\mu_{i+1}^x = [A \ B \ B^d] \mu_i, \quad (13a)$$

$$\Sigma_{i+1}^x = [A \ B \ B^d] \Sigma_i [A \ B \ B^d]^T. \quad (13b)$$

### C. Approximation Methods

In order to define  $\mu_i^d$ ,  $\Sigma_i^d$  and  $\Sigma_i^{zd}$  different approximations of the posterior of a GP from a Gaussian input have been proposed in the literature. In the following, we will give a brief overview of the most commonly used techniques, for details please refer to [7], [8], [9]. For comparison, we furthermore state the computational complexity of these methods under the assumption that  $M > n_z$  and that  $m^a(z)$  and  $k^a(z, z')$ , as well as their derivatives, can be evaluated in  $\mathcal{O}(n_z)$ , which is the case for most common mean and kernel functions.

1) *Mean Equivalent Approximation*: A straightforward and computationally cheap approach is to evaluate (7) at the mean  $\mu_i^z = [\mu_i^x, K_i \mu_i^x]$ , such that

$$\mu_i^d = \mu^d(\mu_i^z), \quad (14a)$$

$$\Sigma_i^d = \Sigma^d(\mu_i^z), \quad (14b)$$

$$\Sigma_i^{zd} = 0. \quad (14c)$$

In [22] it was demonstrated that this can lead to poor approximations for increasing prediction horizons as it neglects the accumulation of uncertainty in the GP. Because  $\Sigma^{zd} = 0$ , this approach furthermore neglects covariance between  $z$  and  $d(z)$  which can severely deteriorate the prediction quality.

The computationally most expensive operation is the matrix multiplication in (6b) for each output dimension of the GP, such that the complexity of one prediction step is  $\mathcal{O}(n_d M^2)$ .

2) *Taylor Approximation*: Using a first-order Taylor approximation of (7), the expected value, variance and covariance of the resulting distribution results in

$$\mu_i^d = \mu^d(\mu_i^z), \quad (15a)$$

$$\Sigma_i^d = \Sigma^d(\mu_i^z) + \nabla \mu^d(\mu_i^z) \Sigma_i^z (\nabla \mu^d(\mu_i^z))^T, \quad (15b)$$

$$\Sigma_i^{zd} = \Sigma_i^z (\nabla \mu^d(\mu_i^z))^T. \quad (15c)$$

Compared to (14) this leads to correction terms for the posterior variance and covariance, taking into account the gradient of the posterior mean and the variance of the input of the GP.

The computationally most expensive operation is a matrix multiplication required for computation of the gradient  $\nabla \mu^d(\mu_i^z)$ , i.e.  $\nabla_z k_a(\mathbf{z}, z) K^{-1}$ . The complexity of one prediction step therefore amounts to  $\mathcal{O}(n_d n_z M^2)$ . Higher order approximations are similarly possible, however at the expense of an increase in computational effort.

3) *Exact Moment Matching*: It has been shown that for certain mean and kernel functions the first and second moments of the posterior distribution can be analytically computed [7]. The parameters of the Gaussian distribution in (12) are then given by

$$\mu_i^d = \mathbb{E}(d(\mathcal{N}(\mu_i^z, \Sigma_i^z))), \quad (16a)$$

$$\Sigma_i^d = \text{var}(d(\mathcal{N}(\mu_i^z, \Sigma_i^z))), \quad (16b)$$

$$\Sigma_i^{zd} = \text{cov}(\mathcal{N}(\mu_i^z, \Sigma_i^z), d(\mathcal{N}(\mu_i^z, \Sigma_i^z))). \quad (16c)$$

In particular, this is possible for a zero prior mean function and the squared exponential kernel

$$k_{SE}(z, z') = \sigma_f^2 \exp\left(-\frac{1}{2}(z - z')^T \Lambda^{-1}(z - z')\right), \quad (17)$$

where  $\Lambda$  is a diagonal length-scale matrix.

As the procedure exactly matches first and second moments of the posterior distribution, it can be interpreted as an optimal fit of a Gaussian to the true distribution. Note that the model formulation directly allows for the inclusion of linear prior mean functions, as they can be expressed through the linear matrices  $A$  and  $B^d$  in (9). The computational complexity of this approach is  $\mathcal{O}(n_d^2 n_z M^2)$  [9].

All presented approximations scale directly with the input and output dimensions, as well as the number of data points

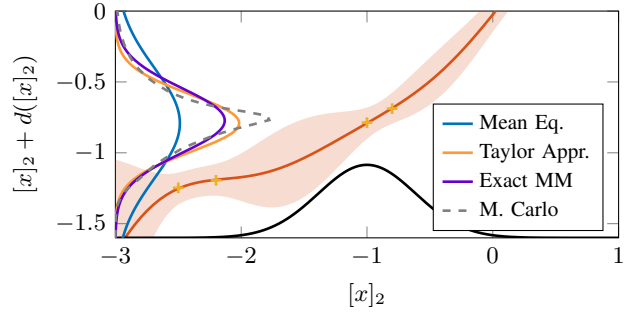


Fig. 2. Comparison of prediction methods for Gaussian input  $[x]_2$ . The posterior distribution  $[x]_2 + d([x]_2)$  is evaluated with the different approximation methods of Section III-C. For reference, the true distribution is approximated by Monte Carlo simulation.

and thus become expensive to evaluate for high dimensional spaces. This limits existing predictive control approaches with GP models to relatively small and slow systems [10], [13], but can be overcome when the nonlinearity depends on only a subset of states and inputs, enabled by the use of nominal models.

**Proposition 1.** *With only slight notational changes, the presented approximation methods similarly apply to prior mean and kernel functions that are functions of only a subset of states and inputs.*

For the *Mean Equivalent* and *Taylor Approximation* this can be seen from (14) and (15), as  $\mu^d(z)$  can be directly evaluated on the subset. For moment matching, the proposition is proven in Appendix A. Evaluating the GP on a subset of states and inputs enables learning of only specific nonlinear effects.

**Remark 2.** *Taking advantage of Proposition 1 can significantly reduce the computational burden, both by requiring less training points  $M$  and by reducing the effective input dimension  $n_z$ .*

In Fig. 2 the different approximation methods are compared for a one-step prediction of the GP shown in Fig. 1 with Gaussian input. As evident, the predictions with *Taylor Approximation* and *Moment Matching* are qualitatively similar, which will typically be the case if the second derivative of the posterior mean and the change of posterior variance of the GP is small over the input distribution. It is furthermore apparent that the posterior distribution is not Gaussian and that the approximation as a Gaussian distribution leads to prediction error, even if the first two moments are matched exactly. This can lead to the effect that locally the *Taylor Approximation* provides a closer fit to the underlying distribution. The *Mean Equivalent Approximation* is very conservative by neglecting the covariance between  $[x]_2$  and  $d([x]_2)$ . Note that depending on the sign of the covariance it can also be overly confident.

#### D. Chance Constraint Formulation

The tractable Gaussian approximation of the state and input distribution over the prediction horizon in (12) obtained from any of the techniques discussed in Section III-C can be used to approximate the chance constraints in (10e) and (10f).

For brevity, we concentrate on state constraints, as input constraints can be treated analogously.

With the Gaussian approximations and the definition of the polytopic constraint region (2), the state chance constraint (10e) can be approximated as

$$P(\mathcal{N}(H^x \mu_i^x, H^x \Sigma_i^x (H^x)^T) < b^x) > 1 - \epsilon^x. \quad (18)$$

Evaluating this probability involves the integration of multivariate Gaussians, which is not analytically tractable. Numerical evaluation of the expression is possible, but is often hard to encompass in optimization procedures, as the evaluation is expensive and analytic derivative information is typically not available [23].

Because of these drawbacks, joint chance constraints of the form (18) are often reduced to more conservative individual chance constraints using ellipsoidal relaxation [24] or Boole's inequality:

$$\begin{aligned} & P(\mathcal{N}(H^x \mu_i^x, H^x \Sigma_i^x (H^x)^T) < b^x) \\ & \leq \sum_{j=1}^p P(\mathcal{N}([H^x]_j \mu_i^x, [H^x]_j \Sigma_i^x [H^x]_j^T) < [b^x]_j). \end{aligned} \quad (19)$$

Constraints on these individual probabilities can be expressed in terms of  $\mu_i^x$  and  $\Sigma_i^x$  through the equivalence

$$\begin{aligned} & P(\mathcal{N}([H^x]_j \mu_i^x, [H^x]_j \Sigma_i^x [H^x]_j^T) < [b^x]_j) \geq 1 - \epsilon_j^x \\ & \Leftrightarrow [H^x]_j \mu_i^x + r_j^x \sqrt{[H^x]_j \Sigma_i^x [H^x]_j^T} \leq [b^x]_j, \end{aligned} \quad (20)$$

with  $r_j^x = \Phi^{-1}(1 - \epsilon_j^x)$ , where  $\Phi^{-1}(\cdot)$  denotes the quantile function of the standard normal distribution. While  $\Phi^{-1}(\cdot)$  cannot be computed analytically, approximations and look-up tables are commonly available and  $r_j^x$  can be evaluated offline. Analogous treatment of the input chance constraint results in

$$[H^u]_j \cdot (K_i \mu_i^u + v_i) + r_j^u \sqrt{[H^u]_j \cdot K_i \Sigma_i^u K_i^T [H^u]_j^T} \leq [b^u]_j. \quad (21)$$

**Remark 3.** Choosing  $r^x$  and  $r^u$  such that joint constraint violation probabilities are guaranteed, e.g. through (19), can lead to undesired and conservative individual constraints [25]. Instead, it is often beneficial to directly constrain the probability of individual constraint violation, offering an interpretation similar to constraint tightening in robust MPC.

When using the Mean Equivalent or Taylor Approximation (see Section III-C) for uncertainty propagation it is possible to decompose the covariance matrix  $\Sigma_i^x = S_i^x S_i^{xT}$  and write the variance update in (13b) in terms of  $S_i^x$  as

$$S_{i+1}^x = [A \quad B \quad B^d] S_i, \quad (22)$$

where  $S_i$  is the decomposition matrix of  $\Sigma_i$ , i.e.  $\Sigma_i = S_i S_i^T$ . Note that the column size of  $S_i^x$  increases in every prediction time step by  $n_d$ . To the best of our knowledge, this is not possible in the case of *Exact Moment Matching*. Details on the decomposition are provided in Appendix B. The constraints can thus be expressed as

$$[H^x]_j \mu_i^x + r_j^x \|[H^x]_j \cdot S_i^x\|_2 \leq [b^x]_j, \quad (23a)$$

$$[H^u]_j \cdot (K_i \mu_i^u + v_i) + r_j^u \|[H^u]_j \cdot K_i S_i^u\|_2 \leq [b^u]_j. \quad (23b)$$

For  $r_j^x, r_j^u > 0$ , corresponding to probabilities of violation under 50 %, these are *convex second-order cone constraints*.

### E. Cost Function

Given the normal distribution of state and input, a number of cost functions can readily be expressed in terms of  $\mu_i^x, \Sigma_i^x$  and  $v_i$ . We briefly discuss some common cost functions and their adaptation to the proposed framework. Using appropriate weighting matrices  $P, Q$  and  $R$  these stage and terminal costs can be defined as

$$l_f(x_{N|k}) = c_{(\cdot)}(x_{N|k}, P), \quad (24a)$$

$$l(x_{i|k}, u_{i|k}) = c_{(\cdot)}(x_{i|k}, Q) + c_{(\cdot)}(u_{i|k}, R), \quad (24b)$$

with  $c_{(\cdot)}$  given e.g. by one of the options outlined below.

a) *Expected Value of Quadratic Cost:* The most common cost in MPC is a weighted quadratic cost on states and inputs. For a normally distributed vector  $\xi$  and weight matrix  $M$  the expected value of a quadratic form is

$$c_q(\xi, M) = \mathbb{E}[\|\xi\|_M^2] = \|\mu^\xi\|_M^2 + \text{tr}(M \Sigma^\xi). \quad (25)$$

For  $M \succeq 0$ , this is a convex function in  $\mu^\xi$  and  $\Sigma^\xi$ .

b) *Risk Weighted Quadratic Cost:* The expected value of a quadratic cost can be adapted to put emphasis on the uncertainty, and adjust the level of cautiousness of the controller. This can e.g. be realized via a weighting factor on the deviation from the mean i.e.

$$\begin{aligned} c_r^s(\xi, M) &= \mathbb{E}[\|\xi + (s-1)(\xi - \mu^\xi)\|_M^2] \\ &= \|\mu^\xi\|_M^2 + s \text{tr}(M \Sigma^\xi), \end{aligned} \quad (26)$$

where  $s-1$  is the weighting factor and  $s \geq 0$ . For  $M \succeq 0$ , function (26) is convex.

**Remark 4.** With  $s = 0$  and  $r^x = r^u = 0$ , this includes the case of certainty equivalent control.

c) *Expected Value of Saturating Cost:* With little data and high uncertainty, a saturating cost has been observed to benefit exploration—especially with respect to online controller learning [9]. With slight modifications, a generalized saturating cost can be formulated as

$$\begin{aligned} c_s(\xi, M) &= \mathbb{E}[1 - \exp(-\|\xi\|_M^2)] \\ &= 1 - |I + 2\Sigma^\xi M|^{-\frac{1}{2}} \exp(-\|\mu^\xi\|_S), \end{aligned} \quad (27a)$$

$$S := M(I + 2\Sigma^\xi M)^{-1}. \quad (27b)$$

### F. Tractable MPC Formulation with GP Model

By utilizing the approximations of the model prediction, the constraints and the cost presented in Sections A to E, the

following general tractable approximation of the MPC problem (10) can be derived:

$$\min_{V, \mu^x, \Sigma^x} l_f(\mu_N^x, \Sigma_N^x) + \sum_{i=0}^{N-1} l(\mu_i^x, \Sigma_i^x, v_i) \quad (28a)$$

$$\text{s.t. } \mu_0^x = x_k \quad (28b)$$

$$\Sigma_0^x = 0 \quad (28c)$$

$$\mu_{i+1}^x = [A \ B \ B^d] \mu_i \quad (28d)$$

$$\Sigma_{i+1}^x = [A \ B \ B^d] \Sigma_i [A \ B \ B^d]^T \quad (28e)$$

$$\mu_i, \Sigma_i \text{ acc. to (12)} \quad (28f)$$

$$\mu_i^d, \Sigma_i^d, \Sigma_i^{zd} \text{ acc. to (14), (15) or (16)} \quad (28g)$$

$$(20), \forall j = 1, \dots, p \quad (28h)$$

$$(21), \forall j = 1, \dots, l, \quad (28i)$$

for  $i = 0, \dots, N-1$ . The resulting optimal control law is obtained in a receding horizon fashion as  $\kappa(x_k) = K_0 x_k + v_0^*(x_k)$ , where  $v_0^*(x_k)$  is obtained by solving (28) for every state  $x_k$ .

**Remark 5.** *In order to employ the convex inequality constraints (23) instead of (20) and (21), constraints and variance dynamics can be reformulated in terms of  $S_i$  instead of  $\Sigma_i$ .*

### G. Computation

The presented formulation of the MPC problem with a GP-based model results in a non-convex optimization problem. At the expense of additional variables, employing Remark 5 can ensure convex inequality constraints. The system dynamics, however, are inherently nonlinear. Assuming twice differentiability of kernel and prior mean function, second order derivative information of all quantities is available. Problems of this form can typically be solved to local optima using Sequential Quadratic Programming (SQP) or nonlinear interior-point methods [26].

There exist a number of general-purpose solvers that can be applied to solve this class of optimization problems, e.g. SNOPT [27], KNITRO [28] or the openly available IPOPT [29]. In addition, there are specialized solvers that exploit the structure of predictive control problems, such as ACADO [30] or Forces PRO [31], which implements a nonlinear interior point method. Derivative information can be automatically generated using automated differentiation tools, such as CASADI [32].

## IV. EXAMPLE

In the following, we demonstrate the proposed algorithm and its properties using a simulation example of an autonomous underwater vehicle (AUV).

### A. Setup

We consider the vehicle's depth control for which we take a nonlinear continuous model of the vehicle at constant surge velocity as ground truth and for simulation purposes [33]. Around a trim point of purely horizontal movement the states and input of the system are

|         |  |
|---------|--|
| $[x]_1$ | the heave velocity relative to trim point [m/s],     |
| $[x]_2$ | the pitch velocity [rad/s],                          |
| $[x]_3$ | the pitch angle relative to trim point [rad],        |
| $u$     | the stern rudder deflection around trim point [rad], |

and the model can be decomposed into a linear and nonlinear part

$$\dot{x} = A_c x + B_c u + B_c^d (g_c([x]_1, [x]_2) + w_c), \quad (29)$$

where  $g_c(0) = 0$  and  $\nabla g_c(0) = 0$ .  $B_c^d = [I, 0]$  specifies the range of the nonlinearities, i.e. that they only affect the velocities and not the integration. We consider white process noise with power spectral density  $PSD = \text{diag}(4 \cdot 10^{-4}, 4 \cdot 10^{-3})$ , which, for simulation purposes, we discretize as  $w_c(t) \sim \mathcal{N}(0, PSD/T_s)$ , for  $kT_s \leq t < (k+1)T_s$ , where  $T_s$  is the sampling time of the discrete-time model. Details of the simulation model are provided in Appendix C.

For the control of the system, we assume knowledge of the linear part of the system model in horizontal position given by  $A_c$ , which in practice can be established using methods of linear system identification around the trim point of the system. We furthermore make an assumption on the structure of the nonlinearity, that is the range of  $B_c^d$  and that  $g_c([x]_1, [x]_2)$  is a function of only the first two states, which follows directly from physical considerations. In order to translate (29) to discrete-time, we use a zero-order hold discretization of the linear part of the model with  $T_s = 100\text{ms}$  to obtain  $A, B$  and  $B^d$ . For improved steady-state error, an additional error state  $[x_{k+1}]_4 = [x_k]_4 + T_s \sum_{i=1}^3 [x_k]_i$  is introduced, and we assume  $w_k$  with  $\Sigma^w = \text{diag}(0.0025^2, 0.025^2)$  in order to capture the process noise and discretization error. A discrete-time representation of the system is then given by

$$x_{k+1} = Ax_k + Bu_k + B^d (g([x_k]_1, [x_k]_2) + w_k), \quad (30)$$

which is in the form of (1). Note that eigenvalues of  $A$  are given by  $\lambda = [1.1, 1.03, 1, 0.727]$ , i.e. the linear system has one integrating and two unstable modes.

### B. Model Learning and Controller Design

We exploit the structure of the nonlinearity and reduce the space of inputs of the GP to the span of  $[x]_1$  and  $[x]_2$ . In addition, due to the structure of  $B^d$ , we consider a two dimensional output. GP output data  $\Delta^1, \Delta^2$  is generated by calculating the deviation of the linear model from the measured states, as described in Section II-C. We employ a squared exponential kernel (17) for both output dimensions with fixed hyperparameters  $\Lambda^1 = \Lambda^2 = \text{diag}(0.35, 0.15)$ , and variances  $\sigma_f^1 = 0.2$  and  $\sigma_f^2 = 0.5$ . These are typically found through hyperparameter optimization given data and prior knowledge about the process.

As ancillary linear controller  $K_i$ , an infinite horizon LQR control law based on the linear nominal model is designed and used it in all prediction steps  $i$ , stabilizing the linear system and reducing the growth of uncertainty over the prediction. The considered weight matrices are

$$Q = \text{diag}([1, 0, 10, 0.5]), \quad R = 20. \quad (31)$$

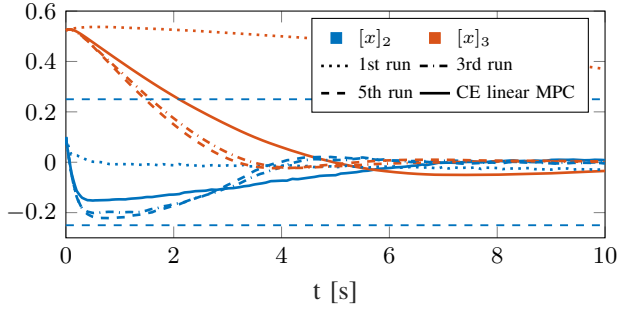


Fig. 3. State trajectories of experiment runs with GP-based MPC and with certainty equivalent linear MPC for comparison. The state constraint on  $[x]_2$  is shown in dashed blue.

To propagate the uncertainties associated with the GP we make use of the *Taylor Approximation* outlined in Section III-C. Constraints are introduced based on Remark 3 considering a maximum probability of individual constraint violation of 2.28%, corresponding to  $r^x = r^u = 2 \forall j$ , i.e. a 2- $\sigma$  confidence bound. A quadratic stage cost as in (25) is selected, with weight matrices as in the ancillary LQR controller (31) and terminal cost according to its infinite horizon cost, i.e.  $P$  is defined as the solution to the associated discrete-time algebraic Riccati equation. The MPC optimization problem (28) is solved using Forces PRO [31].

### C. Batch Learning

We consider a sequence of simulations, where the controller task is to regulate the vehicle to its set point under input and state constraints

$$\mathcal{U} = \{u \in \mathbb{R} \mid -0.233 \leq u \leq 0.465\}, \quad (32a)$$

$$\mathcal{X} = \{x \in \mathbb{R}^4 \mid -0.23 \leq [x]_2 \leq 0.23\}, \quad (32b)$$

corresponding to  $\pm 20^\circ$  maximum deflection of the rudder and a constraint on pitch velocity of  $\pm 13.2^\circ$  per second. From a given initial position of  $x_0 = [0 \ 0.1 \ 0.5236 \ 0]^T$  we simulate the closed-loop system for 10s, corresponding to 100 discrete time steps. By considering every second time step we use the measured data to generate  $M = 50$  data points for the GP in the subsequent run. In the first run, no data is available.

**Remark 6.** *More sophisticated methods can be used to generate the GP data from all measurements, e.g. pseudo inputs or sparse GP approximations [34] to cover a larger part of the training space. For clarity of the exposition, we consider this simple and episodic setup.*

Fig. 3 shows that initially, in the absence of any training data, the control of the system is very cautious as the GP model in the absence of data is given by the prior distribution with large uncertainty. Due to this high uncertainty in the nonlinear dynamics, the chance constraint on  $[x]_2$  is constantly active, hardly allowing the system to pitch down. As the controller learns the dynamics in consecutive runs, the residual model uncertainty decreases and performance improves significantly, both by allowing the system to approach constraints more tightly and by exploiting the nonlinear dynamics of the system. For comparison, the performance with a certainty equivalent

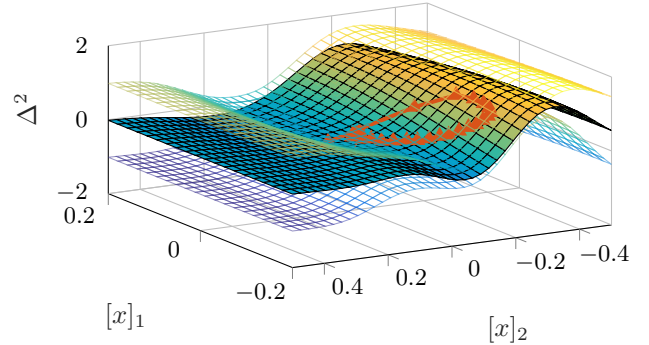


Fig. 4. Exemplary plot of the GP at run 4. The plot shows the posterior mean of the second output dimension  $[\mu^d(z)]_2$  with 2- $\sigma$  bound displayed by the shaded mesh. The red line shows the data points  $\Delta^2$  used in the GP.

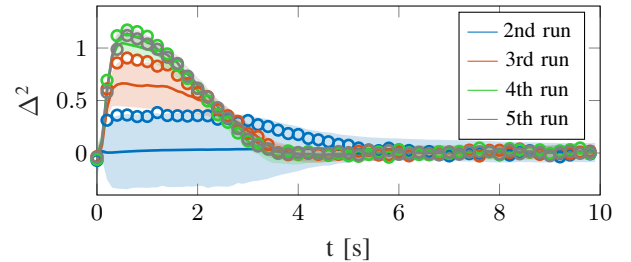


Fig. 5. Second output dimension of GP  $[d(z)]_2$  for runs two to five along the system trajectory. Shaded is the 2- $\sigma$  confidence region and circles indicate data points  $\Delta^2$  generated from state measurements and used in the data set  $\mathcal{D}$  of the following run.

linear MPC controller, which considers no uncertainty or nonlinearities in the system, is also shown. While in the first run the GP-based MPC controller is overly cautious, by the third run it clearly outperforms the linear MPC.

Fig. 4 shows an exemplary plot of the GP used in the experiments, which illustrates the generalization capabilities of the trained GP. We can furthermore see that with increasing distance from input data the posterior distribution returns to the prior mean and high uncertainty. Fig. 5 shows the learning progress of the GP during the first five runs. Plotted is the second output of the posterior mean function  $[\mu^d(z_k)]_2$  with 2- $\sigma$  confidence region according to the posterior variance along the trajectory of each experiment. Markers show the actual deviations from the linear model measured on that trajectory and used as data for the GP in the next run. The uncertainty in prediction is able to capture the true deviation from the model dynamics, and, in later experiments, we achieve an accurate dynamics model with low uncertainty on the considered trajectory.

After highlighting the iterative learning performance, the following results demonstrate the real-time feasibility of the GP-based MPC approach. We repeat the closed-loop simulations for 150 initial conditions drawn uniformly at random from  $\mathcal{X}_0 = \{x \mid |x| \leq [0.15, 0.15, 0.6981, 0]\}$ . Infeasible initial conditions are discarded, resulting in 106 simulations. Each run simulates 10 different noise realizations, an outline of the simulation procedure is given in Algorithm 1. The simulations were carried out on a laptop computer with a 2.6 GHz i7-5600 CPU and 12GB Ram. The MPC optimization problem

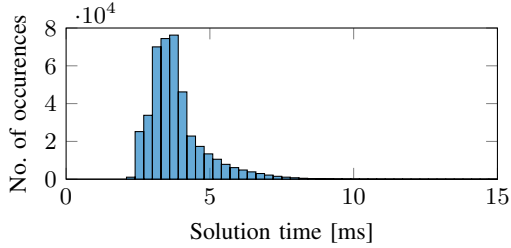


Fig. 6. Histogram of the computation times in batch learning simulations.

was solved on average in 3.9 ms and at most in 87.7 ms. As the histogram in Fig. 6 shows, more than 99.9% of solutions were computed in below 10 ms. The closed-loop performance in these simulations is provided in Table I. We can see that performance increases significantly in the first two runs, after which improvements of achieved cost and prediction accuracy are less pronounced. After the initial training run, the approach outperforms the linear MPC also on average for randomized initial conditions.

#### D. Online Learning

With minor modifications of the formulation, the presented approach can also be applied to reference tracking problems. We consider the case of online learning in the following, i.e. the data is continuously updated during the closed-loop run. In the considered scenario, the goal is to track reference changes from the original zero set point to  $x_{ref,1} = [0.036, 0, 0.555, 0]$ ,  $u_{ref,1} = -0.0625$  and then  $x_{ref,2} = [0.06, 0, 0.817, 0]$ ,  $u_{ref,2} = -0.078$ , corresponding to pitch angles of  $30^\circ$  and  $45^\circ$ , respectively. We furthermore consider a safety state constraint on the pitch angle of at least  $10^\circ$  below the reference and input constraints as before. To enable fast changes of the reference, a small weight is chosen on the error state, with  $Q = \text{diag}([1, 0, 10, 10^{-4}])$  and the prediction horizon is increased to  $N = 30$ .

We consider  $M = 30$  data points, which are updated at every 10th time step with the current measurement, while the oldest training point is dropped. The training data is initialized with 30 data points of zero input and zero output. For comparison, we run the same simulation with a soft constrained linear MPC formulation with the same cost function, which does not consider nonlinearities or uncertainties in the dynamics. Fig. 7 shows the results demonstrating improved performance of the GP-based MPC controller over the linear MPC. This is

---

#### Algorithm 1 Simulation Procedure

---

- 1: **for**  $i = 1 : 150$  **do** ▷ No. initial conditions
  - 2:   draw initial condition  $x_{0,i} \in \mathcal{X}_0$  uniformly at random
  - 3:   set GP Dataset  $\mathcal{D}_{i,0} = \emptyset$
  - 4:   **for**  $j = 1 : 5$  **do** ▷ No. consecutive runs
  - 5:     **for**  $k = 1 : 10$  **do** ▷ No. disturbance realizations
  - 6:      run simulation  $\mathcal{S}_{i,j,k}$
  - 7:     **end for**
  - 8:     Set  $\mathcal{D}_{i,j}$  according to  $\mathcal{S}_{i,j,1}$
  - 9:   **end for**
  - 10: **end for**
- 

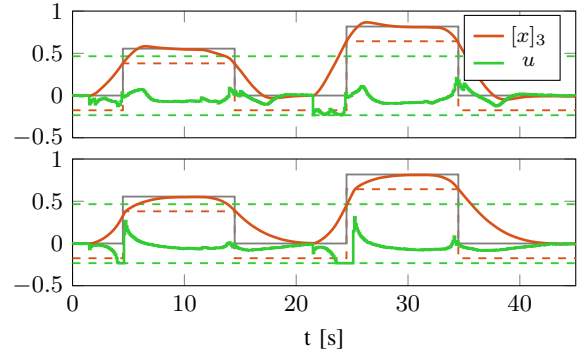


Fig. 7. Comparison of online Learning GP-based MPC (top) and linear certainty equivalent MPC (bottom). In solid gray the reference value of the pitch angle, dashed in the respective color the state and input constraints.

especially true with regard to the safety constraint, which is violated under the linear MPC control law even though the soft constraint is chosen as an exact penalty function such that constraints are always satisfied, if possible.

#### V. CONCLUSION

This paper demonstrated the use of Gaussian process regression to learn nonlinearities for improved performance in model predictive control. Combining GP dynamics with a linear system enables a less conservative treatment in particular of unstable systems by incorporating a linear state feedback controller that reduces uncertainty growth along the prediction horizon. The formulation allows for learning only parts of the dynamics, which is key for keeping the required number of data points and computational complexity of the GP regression feasible for online control. Approximation methods for the propagation of the state distributions over the prediction horizon were reviewed and it was shown how this enables a principled treatment of chance constraints on both states and inputs.

Simulation examples have illustrated how the proposed formulations provides cautious control with improved performance of a medium-sized system and in particular have demonstrated that sub-second sampling times can be achieved, moving the use of Gaussian-processes in MPC in the range of real-time control.

TABLE I  
MEAN CLOSED-LOOP COST AND PREDICTION ERROR.

| GP-based, run no. | $\bar{J}$ | $\bar{e}$ |
|-------------------|-----------|-----------|
| 1                 | 105.5     | 0.0113    |
| 2                 | 26.78     | 0.0060    |
| 3                 | 23.34     | 0.0017    |
| 4                 | 23.28     | 0.0007    |
| 5                 | 23.26     | 0.0006    |
| Linear MPC        | 29.17     | -         |

$$\bar{J} = \text{mean}(\sum_{k=1}^{100} \|x_k\|_Q^2 + \|u_k\|_R^2),$$

$$\bar{e} = \text{mean}(\sum_{k=1}^{100} \|\mu^d(z_k) - \Delta_k\|^2)$$



## APPENDIX A

## EXACT MOMENT MATCHING ON SUBSET OF INPUTS

We partition  $z$  w.l.o.g. in  $z = [\tilde{z}, \bar{z}]$ , such that  $d$  is a function of  $\tilde{z}$  only. We can compute expectation and variance of  $d(\tilde{z})$  using the marginal distribution  $\tilde{z} \sim \mathcal{N}(\mu^{\tilde{z}}, \Sigma^{\tilde{z}})$  by applying techniques similar to those used e.g. in [9]. This yields  $\mu^d = \mathbb{E}_{d,\tilde{z}}(d(\tilde{z}))$ ,  $\Sigma^d = \text{var}_{d,\tilde{z}}(d(\tilde{z}))$ , where the subscripts indicate with respect to which random variable the expectation is taken. For the covariance we have

$$\begin{aligned} \text{cov}(z, d) &= \mathbb{E}_{z,d}(zd(\tilde{z})^T) - \mathbb{E}_z(z)\mathbb{E}_{\tilde{z},d}(d(\tilde{z})) \\ &= \mathbb{E}_{z,d}(zd(\tilde{z})^T) - \mu^z \mu^d. \end{aligned} \quad (33)$$

Using the law of total expectation, we get

$$\begin{aligned} \mathbb{E}_{z,d}(zd(\tilde{z})^T) &= \mathbb{E}_{\tilde{z},d}(\mathbb{E}_z(zd(\tilde{z})^T|\tilde{z},d)) \\ &= \mathbb{E}_{\tilde{z},d}(\mathbb{E}_{\tilde{z}}(z|\tilde{z},d)d(\tilde{z})^T) \\ &= \mathbb{E}_{\tilde{z},d}\left(\left[(\mu^{\tilde{z}} + \Sigma^{\tilde{z}\tilde{z}}(\Sigma^{\tilde{z}})^{-1})(\tilde{z} - \mu^{\tilde{z}})\right]d(\tilde{z})^T\right) \\ &= \left[\Sigma^{\tilde{z}\tilde{z}}(\Sigma^{\tilde{z}})^{-1}\right] \mathbb{E}_{\tilde{z},d}(\tilde{z}d(\tilde{z})^T) \\ &\quad - \left[\mu^{\tilde{z}} - \Sigma^{\tilde{z}\tilde{z}}(\Sigma^{\tilde{z}})^{-1}\mu^{\tilde{z}}\right] \mu^d, \end{aligned} \quad (34)$$

and with  $\text{cov}(\tilde{z}, d(\tilde{z})) = \mathbb{E}_{\tilde{z},d}(\tilde{z}d(\tilde{z})^T) - \mu^{\tilde{z}}\mu^d$  this yields

$$\text{cov}(z, d(\tilde{z})) = \left[\Sigma^{\tilde{z}\tilde{z}}(\Sigma^{\tilde{z}})^{-1}\right] \text{cov}(\tilde{z}, d(\tilde{z})), \quad (35)$$

where  $\text{cov}(\tilde{z}, d(\tilde{z}))$  can again be computed from the marginal distribution. Using (35) we can thus evaluate (16) on a subset of the inputs, by taking into account the covariance of  $\tilde{z}$  with  $\bar{z}$ .

## APPENDIX B

## REFORMULATION OF INDIVIDUAL CHANCE CONSTRAINTS AS SECOND-ORDER CONE CONSTRAINT

$\Sigma_0^x = 0$  can be decomposed as  $S_0^x(S_0^x)^T$  with  $S_0^x = 0_{n \times 1}$ . Given a decomposition of  $\Sigma_i^x = S_i^x(S_i^x)^T$ , we can express

$$\Sigma_i^z = \begin{bmatrix} S_i^x \\ K_i S_i^x \end{bmatrix} \left[ (S_i^x)^T \quad (S_i^x)^T K_i^T \right] = S_i^z (S_i^z)^T. \quad (36)$$

Given  $S_i^z$  and  $S_i^d = \sqrt{\Sigma^d(\mu_i^{\tilde{z}})}$ , we find for  $\Sigma_i$ :

a) *Mean Equivalent:*

$$\Sigma_i = \begin{bmatrix} S_i^z & 0 \\ 0 & S_i^d \end{bmatrix} \begin{bmatrix} (S_i^z)^T & 0 \\ 0 & (S_i^d)^T \end{bmatrix}, \quad (37)$$

b) *Taylor Approximation:*

$$\Sigma_i = \begin{bmatrix} S_i^z & 0 \\ \nabla \mu^d(\mu_i^{\tilde{z}}) S_i^z & S_i^d \end{bmatrix} \begin{bmatrix} (S_i^z)^T & (S_i^z)^T (\nabla \mu^d(\mu_i^{\tilde{z}}))^T \\ 0 & (S_i^d)^T \end{bmatrix}. \quad (38)$$

The update equation according to (28e) is then

$$S_{i+1}^x = [A \quad B \quad B^d] S_i. \quad (39)$$

Given  $S_i^x$ , (20) and (21) can be reformulated for each  $j$  as

$$[H^x]_j \cdot \mu_i^x + r_j^x \|[H^x]_j \cdot S_i^x\|_2 \leq [b^x]_j, \quad (40)$$

The input constraints can be reformulated analogously.

APPENDIX C  
SIMULATION MODEL

The nonlinear simulation model can be expressed as

$$\begin{bmatrix} \dot{w} \\ \dot{q} \\ \dot{\Theta} \end{bmatrix} = M^{-1} \left( \begin{bmatrix} Z_{uw}u_0 & (Z_{uq} + m)u_0 & 0 \\ M_{uw}u_0 & M_{uq}u_0 & -z_G W \\ 0 & 1 & 0 \end{bmatrix} \begin{bmatrix} w \\ q \\ \Theta \end{bmatrix} + \begin{bmatrix} Z_{w|w}|w|w| + Z_{q|q}|q|q| + m z_G q^2 \\ M_{w|w}|w|w| + M_{q|q}|q|q| - m z_G w q \\ 0 \end{bmatrix} + \begin{bmatrix} Z_{uu}u_0^2 \\ M_{uu}u_0^2 \\ 0 \end{bmatrix} \delta_s \right), \quad (41)$$

with

$$M^{-1} = \begin{bmatrix} [m - Z_{\dot{w}} & -Z_{\dot{q}}]^{-1} & 0 \\ -M_{\dot{w}} & I_{yy} - M_{\dot{q}} & \\ 0 & 0 & 1 \end{bmatrix}$$

and the parameters given in [33]. With constant surge velocity  $u_0 = 2\text{m/s}$ , we trim the model around  $w \cos(\Theta) + u_0 \sin(\Theta) = 0$  and  $q = 0$ . This yields

$$\begin{aligned} w_{trim} &= -0.0633 \text{ m/s}, \\ \Theta_{trim} &= -0.0316 \text{ rad}, \\ \delta_{trim} &= -0.1159 \text{ rad}. \end{aligned}$$

With  $x = [w - w_{trim}, q, \Theta - \Theta_{trim}]$  and  $u = \delta - \delta_{trim}$ , (29) follows.

## REFERENCES

- [1] K. S. Narendra and K. Parthasarathy, "Identification and control of dynamical systems using neural networks," *IEEE Trans. Neural Netw.*, vol. 1, no. 1, pp. 4–27, Mar. 1990.
- [2] K. J. Hunt, D. Sbarbaro, R. Zbikowski, and P. J. Gawthrop, "Neural networks for control systems—a survey," *Automatica*, vol. 28, no. 6, pp. 1083–1112, Nov. 1992.
- [3] D. Nguyen-Tuong and J. Peters, "Model learning for robot control: a survey," *Cognitive Process.*, vol. 12, no. 4, pp. 319–340, Nov. 2011.
- [4] O. Sigaud, C. Salan, and V. Padois, "On-line regression algorithms for learning mechanical models of robots: A survey," *Robotics and Autonomous Syst.*, vol. 59, no. 12, pp. 1115–1129, Dec. 2011.
- [5] G. Pillonetto, F. Dinuzzo, T. Chen, G. De Nicolao, and L. Ljung, "Kernel methods in system identification, machine learning and function estimation: A survey," *Automatica*, vol. 50, no. 3, pp. 657–682, Mar. 2014.
- [6] E. D. Klenske, M. N. Zeilinger, B. Schoelkopf, and P. Hennig, "Gaussian process based predictive control for periodic error correction," *IEEE Trans. Control Syst. Technol.*, vol. 24, pp. 110–121, Jan. 2016.
- [7] J. Quiñero-Candela, A. Girard, and C. E. Rasmussen, "Prediction at an uncertain input for Gaussian processes and relevance vector machines application to multiple-step ahead time-series forecasting," Danish Tech. Univ., Technical Report IMM-2003-18, Oct. 2003.
- [8] M. Kuß, "Gaussian process models for robust regression, classification, and reinforcement learning," Ph.D. dissertation, TU Darmstadt, Darmstadt, Apr. 2006.
- [9] M. Deisenroth, "Efficient reinforcement learning using Gaussian processes," Ph.D. dissertation, KIT, Karlsruhe, Nov. 2010.
- [10] J. Kocijan, R. Murray-Smith, C. Rasmussen, and A. Girard, "Gaussian process model based predictive control," *Proc. Amer. Control Conf.*, pp. 2214–2219, Jun. 2004.
- [11] A. Grancharova, J. Kocijan, and T. A. Johansen, "Explicit stochastic predictive control of combustion plants based on Gaussian process models," *Automatica*, vol. 44, no. 6, pp. 1621–1631, Jun. 2008.
- [12] G. Cao, E. M.-k. Lai, and F. Alam, "Gaussian process model predictive control of unmanned quadrotors," in *Int. Conf. Control, Automation and Robotics*, 2016.
- [13] X. Yang and J. M. Maciejowski, "Fault tolerant control using Gaussian processes and model predictive control," *Int. J. Appl. Math. Comput. Sci.*, vol. 25, no. 1, pp. 133–148, Mar. 2015.

- [14] C. J. Ostafew, J. Collier, A. P. Schoellig, and T. D. Barfoot, "Learning-based nonlinear model predictive control to improve vision-based mobile robot path tracking," *J. Field Robotics*, vol. 33, no. 1, pp. 133–152, 2015.
- [15] C. J. Ostafew, A. P. Schoellig, and T. D. Barfoot, "Robust constrained learning-based NMPC enabling reliable mobile robot path tracking," *Int. J. Robotics Research*, vol. 35, no. 13, pp. 1547–1563, 2016.
- [16] M. P. Deisenroth, M. F. Huber, and U. D. Hanebeck, "Analytic moment-based Gaussian process filtering," in *Proc. 26th Annu. Int. Conf. Mach. Learning*, Montreal, Canada, 2009, pp. 225–232.
- [17] D. Martino Raimondo, D. Limon, M. Lazar, L. Magni, and E. F. Camacho, "Min-max model predictive control of nonlinear systems: A unifying overview on stability," *European J. Control*, vol. 15, no. 1, pp. 5–21, 2009.
- [18] M. Cannon, B. Kouvaritakis, S. V. Rakovic, and Q. Cheng, "Stochastic tubes in model predictive control with probabilistic constraints," *IEEE Trans. Automat. Control*, vol. 56, no. 1, pp. 194–200, Jan. 2011.
- [19] J. B. Rawlings and D. Mayne, *Model Predictive Control: Theory and Design*. Madison, WI: Nob Hill Publishing, 2009.
- [20] L. Magni, G. De Nicolao, R. Scattolini, and F. Allgöwer, "Robust model predictive control for nonlinear discrete-time systems," *Int. J. Robust and Nonlinear Control*, vol. 13, no. 3-4, pp. 229–246, Feb. 2003.
- [21] A. Bemporad and M. Morari, "Robust model predictive control: A survey," *Robustness in Identification and Control*, vol. 245, pp. 207–226, 1999.
- [22] A. Girard, C. E. Rasmussen, and R. Murray-Smith, "Gaussian process priors with uncertain inputs : Multiple-step-ahead prediction," Univ. Glasgow, Glasgow, Technical Report TR-2002-119, 2002.
- [23] J. P. Cunningham, P. Hennig, and S. Lacoste-Julien, "Gaussian probabilities and expectation propagation," *arXiv:1111.6832*, Nov. 2013.
- [24] D. H. van Hessem and O. H. Bosgra, "Closed-loop stochastic dynamic process optimization under input and state constraints," *Proc. Amer. Control Conf.*, pp. 2023–2028, May 2002.
- [25] M. Lorenzen, F. Dabbene, R. Tempo, and F. Allgöwer, "Constraint-tightening and stability in stochastic model predictive control," *arXiv:1511.03488*, Nov. 2015.
- [26] M. Diehl, H. J. Ferreau, and N. Haverbeke, "Efficient numerical methods for nonlinear mpc and moving horizon estimation," in *Nonlinear Model Predictive Control*, ser. Lecture notes in control and information sciences. Springer Berlin Heidelberg, 2009, vol. 384, pp. 391–417.
- [27] P. E. Gill, W. Murray, and M. A. Saunders, "SNOPT: An SQP algorithm for large-scale constrained optimization," *SIAM J. Optimization*, vol. 47, no. 1, pp. 99–131, 2005.
- [28] R. H. Byrd, J. Nocedal, and R. A. Waltz, "Knitro: An integrated package for nonlinear optimization," in *Large-Scale Nonlinear Optimization*. Boston, MA: Springer US, 2006, pp. 35–59.
- [29] A. Wächter and L. T. Biegler, "On the implementation of an interior-point filter line-search algorithm for large-scale nonlinear programming," *Math. Programming*, vol. 106, no. 1, pp. 25–57, Mar. 2006.
- [30] B. Houska, H. J. Ferreau, and M. Diehl, "ACADO toolkit – an open source framework for automatic control and dynamic optimization," *Optimal Contr. Applicat. and Methods*, vol. 32, no. 3, pp. 298–312, May 2011.
- [31] A. Domahidi and J. Jerez, "FORCES Professional," embotech GmbH (<http://embotech.com/FORCES-Pro>), Jul. 2014.
- [32] J. Andersson, "A general-purpose software framework for dynamic optimization," Ph.D. dissertation, KU Leuven, Leuven, Oct. 2013.
- [33] M. S. Naik and S. N. Singh, "State-dependent Riccati equation-based robust dive plane control of AUV with control constraints," *Ocean Eng.*, vol. 34, no. 11-12, pp. 1711–1723, Aug. 2007.
- [34] J. Quiñero-Candela, C. E. Rasmussen, and R. Herbrich, "A unifying view of sparse approximate Gaussian process regression," *J. Mach. Learning Res.*, vol. 6, pp. 1935–1959, Dec. 2005.